

In situ doping of graphene by exfoliation in a nitrogen ambient

Cite as: Appl. Phys. Lett. **98**, 113115 (2011); <https://doi.org/10.1063/1.3562018>

Submitted: 31 December 2010 . Accepted: 05 February 2011 . Published Online: 17 March 2011

Kevin Brenner, and Raghu Murali



View Online



Export Citation

ARTICLES YOU MAY BE INTERESTED IN

[Single step, complementary doping of graphene](#)

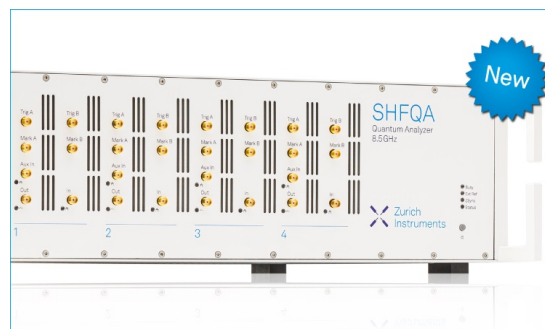
Applied Physics Letters **96**, 063104 (2010); <https://doi.org/10.1063/1.3308482>

[Controllable graphene N-doping with ammonia plasma](#)

Applied Physics Letters **96**, 133110 (2010); <https://doi.org/10.1063/1.3368697>

[Breakdown current density of graphene nanoribbons](#)

Applied Physics Letters **94**, 243114 (2009); <https://doi.org/10.1063/1.3147183>



Your Qubits. Measured.

Meet the next generation of quantum analyzers

- Readout for up to 64 qubits
- Operation at up to 8.5 GHz, mixer-calibration-free
- Signal optimization with minimal latency

Find out more



In situ doping of graphene by exfoliation in a nitrogen ambient

Kevin Brenner and Raghu Murali^{a)}

Nanotechnology Research Center, Georgia Institute of Technology, 791 Atlantic Drive, Atlanta, Georgia 30332, USA

(Received 31 December 2010; accepted 5 February 2011; published online 17 March 2011)

We present an *in situ* method of n-doping graphene by exfoliating in an N-ambient. By exfoliating single-layer graphene in a nitrogen-rich environment, the dopant specie plays an active role in minimizing C–C reconstruction that typically occurs at the moment of defect generation. Employing such *in situ* methods provides an efficient mechanism of passivating defects produced during graphene growth and transfer, as well as a means of controllably incorporating dopant species into the graphene lattice. © 2011 American Institute of Physics. [doi:10.1063/1.3562018]

Graphene, a single layer of sp^2 hybridized carbon atoms, has gained increasing interest as a candidate for nanoscale devices, exhibiting ultrahigh mobility¹ and tunable carrier concentration.² Being an atomically thin system, innovative methods for controlled and efficient embedding of dopant species into the graphene lattice are needed to optimize its conductance at nanoscale dimensions. During “*in situ*” doping, we aim to introduce dopant species during either the *growth* or *transfer* step. Graphene growth, either by sublimation of Si from SiC (Ref. 3) or chemical-vapor deposition (CVD) (Ref. 4) can provide unique avenues for doping graphene, where passivation of fresh defect sites can occur at the time of generation. Postgrowth, graphene can be transferred to arbitrary substrates and is an attractive method to obtain large-area graphene sheets. In this work, graphene is exfoliated in nitrogen ambient to induce n-type doping, and demonstrates the possibility of doping graphene during the transfer process.

A number of doping methods for graphene have been previously explored, the majority of which have focused on surface charge transfer to the graphene sheet. These doping methods have been shown to have a relatively weak charge contribution, about 0.003 carriers per basal atom,⁵ typically limiting the induced carrier concentrations to around 10^{12} cm⁻². Doping from adsorption of gaseous oxygen and water vapor,² ammonia,⁶ and carbon monoxide⁷ have been previously explored. Doping from charge transfer of films of various metals,^{8,9} polymer electrolytes,¹⁰ diazonium salts,¹¹ aromatic molecules,¹² and polyethyleneimine¹³ have been explored. It has been previously suggested¹⁴ that nitrogen edge functionalization, by means of electrically annealing graphene nanoribbons in an ammonia environment is capable of inducing moderate n-type carrier concentrations. Similar methods of n-type doping through nitrogen defect passivation on the basal plane of graphene sheets have been probed by reduction in graphene oxide in an ammonia environment,¹⁵ introduction of ammonia to the CVD growth process,¹⁶ arc discharge in an H₂ and ammonia environment¹⁷ and exposure to a low-power ammonia plasma.¹⁸ Most previous methods rely on postgrowth doping, which is inherently weaker than the *in situ* doping method demonstrated in this work. In addition, in some of these methods, increased carrier concentration comes at the cost

of an increased basal plane defect density, characterized by the emergence of a prominent D-peak¹⁹ during Raman imaging and poor mobilities of 200–400 cm²/V s.¹⁶

Graphene devices in this work are exfoliated (from Kish graphite) onto 300 nm of thermally grown SiO₂ on highly-doped silicon (to serve as a back-gate). Cleaning of the substrate is performed prior to exfoliation—the substrate is baked for 1 h at 400 °C in a nitrogen ambient (N-ambient). An N-ambient is produced using a Terra Universal Dual Purge system. Relative humidity is monitored *in situ* and kept below 5% using a 4700 SCCM (SCCM denotes cubic centimeter per minute at STP) high-flow purge of N₂. An internal positive pressure of ~180 mT is maintained. Exfoliation of the graphene sheets is carried out in the same N-ambient, without removal of the substrate, using a procedure similar to exfoliation in air.² The substrate is then removed from the N-ambient and monolayer and few-layer graphene devices are identified optically and verified using Raman spectroscopy. All processing steps postexfoliation are kept below 200 °C to ensure that nitrogen passivated bonds remain intact. Nitrogen passivation has been previously probed²⁰ using x-ray photoelectron spectroscopy and shown to have binding energies on the order of 400 eV, making it robust throughout the processing temperatures used in this work. Contact metallization is patterned using electron beam lithography and a metal evaporation of Ti/Au (20 nm/80 nm) followed by a liftoff procedure. The devices are then pumped for 24 h at a pressure of 1.5×10^{-5} Torr before performing four-point electrical testing under vacuum. A pulsed gating technique²¹ is used to minimize hysteresis from previous gate sweeps and identify true values for the minimum conductivity point ($V_{g \text{ min}}$). A double-sweep of the gate voltage is performed on all devices to verify the suppression of the hysteresis and $V_{g \text{ min}}$ stability with multiple sweeps. Scanning electron microscope (SEM) images are taken postelectrical testing to determine graphene flake widths.

Electrical testing results of two representative devices are shown in Fig. 1(a)—these devices are on the same substrate; both devices are n-doped but the carrier concentration at zero gate bias is different between the two. The corresponding SEM images of the graphene flakes are shown in Fig. 1(b). The devices are found to exhibit mobilities in excess of 5000 cm²/V s. Raman spectroscopy is performed on the graphene basal plane Fig. 1(c). The lack of a D-peak for

^{a)}Electronic mail: raghu@gatech.edu. Tel.: 404 385 6463.

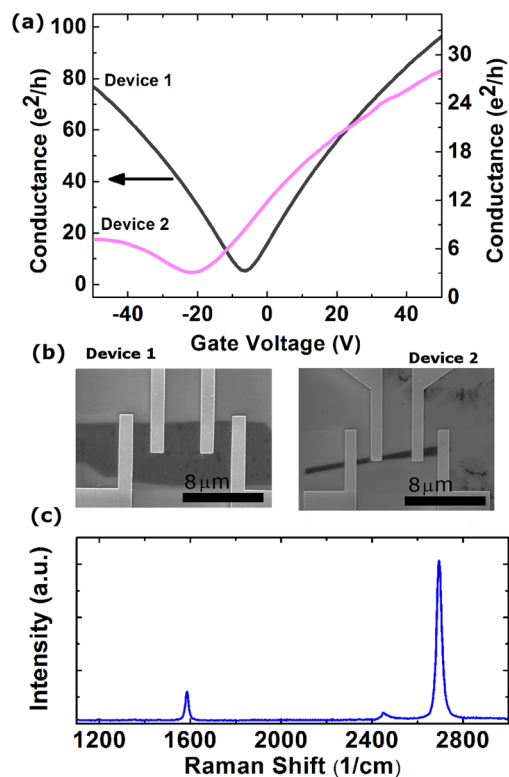


FIG. 1. (Color online) (a) Four-point electrical data from two devices post-exfoliation in a nitrogen environment. The devices exhibit $V_{g \min}$ locations of -23 V and -7 V for Device 1 and 2, respectively. (b) SEM images of the graphene flakes for Device 1 and 2 revealing widths of $1 \mu\text{m}$ and $6 \mu\text{m}$, respectively. The narrower line-width of Device 2 is found to exhibit a larger n-type shift. All SEM images are taken postelectrical testing (c) Raman spectroscopy is performed on the basal plane of all devices. The absence of a D-peak indicates that the exfoliation process maintains the crystalline quality of the graphene ribbon, and that the edge is the primary source of charge donation.

the devices studied in this work indicates that a pristine basal plane, with minimal defect density, is maintained when using this method.

Multiple *in situ* doped graphene devices across four separate process batches are fabricated and tested for their electrical response. Electrical measurements of all devices reveal n-doped graphene, from the negative values of $V_{g \min}$, Fig. 2(a). The position of $V_{g \min}$ as a function of flake width is plotted, Fig. 2(b). A trend of increased n-type doping with reduced flake dimensions is observed for all devices within a batch, indicated by dashed lines. Since the number of edge dopant species remains fixed with width scaling, an increasing n-type carrier concentration is observed. The n-type doping of graphene ribbons (GR) is attributed to nitrogen passivation of dangling σ -bonds along the ribbon edge—these dangling bonds are thought to occur at the time of cleaving during the exfoliation process. It can be seen that there is a small $V_{g \min}$ offset between substrates. This variation is attributed to basal plane doping from process-related residues which, despite thorough cleaning, induce a small background doping level. Though this doping offset varies between process batches, it is reasonable to assume that it remains fixed within a single batch since the substrate and all devices fabricated atop it are exposed to identical process conditions. Additionally, devices of similar widths but within the same substrate exhibit comparable doping, indicating little spatial variation in doping within a given substrate.

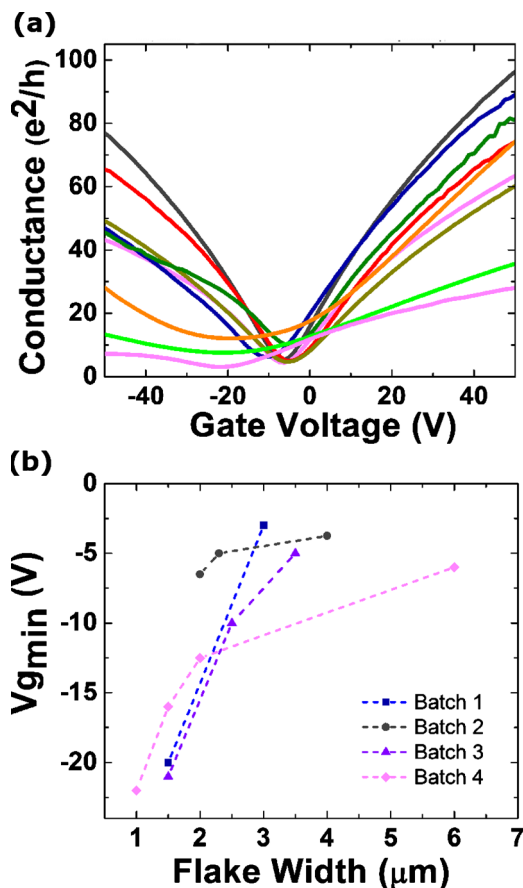


FIG. 2. (Color online) The location of $V_{g \min}$ for graphene devices exfoliated in a nitrogen environment. (a) The resulting electrical testing of multiple *in situ* doped graphene devices, fabricated across four separate process batches. The different locations of $V_{g \min}$ are attributed to variations in flake widths. Devices exhibit mobilities ranging from 1000 – $7000 \text{ cm}^2/\text{V s}$. (b) The position of $V_{g \min}$ for *in situ* doped devices as a function of flake width. A trend of increased n-type doping, indicated by a negative shift in $V_{g \min}$, with reduced flake width is observed for all devices within a batch (indicated by a dashed-line). This shift is attributed to the increasing carrier concentration donated by the ribbon edge. Since the number of edge atoms, and consequently carriers donated by the edge, remains fixed as the ribbon width is reduced, the carrier concentration from the edge increases.

Graphene defect sites can undergo various C–C reconstructions in an attempt to form a stable lattice. In terms of defect passivation with foreign elements, zigzag edges are of greater significance than armchair edges due to their large density of states near the Fermi level.^{22–26} This has been verified experimentally through scanning tunneling microscopy imaging along the edge of graphene sheets.²⁷ Zigzag edges with dangling σ -bonds are not stable and have a natural tendency to undergo reconstruction in the form of two adjacent hexagons transitioning into one heptagon and one pentagon.^{28–31} For this reason, when attempting to passivate defects of fresh graphene vacancies, the choice of element for passivation must provide an energetically favorable alternative to C–C reconstruction. Nitrogen passivation of dangling bonds has been shown to be capable of providing a stable alternative.^{32–34} In addition to this, it has been shown^{32,34} that incorporation of nitrogen into the graphene lattice is most energetically favorable along the ribbon edge, providing *in situ* nitrogen doping with an inherent spatial selectivity of decorating only the edge of the GR. Doping using this method occurs through the generation of pyridinic-N and pyrrolic-N lattices,²⁰ who donate 1 and 2

conducting electrons to the π -system, respectively.

In situ doping of graphene is especially attractive as a counterpart to the growth or transfer of graphene from various substrates (postgrowth) such as SiC, Cu,¹⁶ Ni.³⁵ Defects are currently an unavoidable reality to the fabrication of graphene devices. Defects have been shown to be generated during the growth of epitaxial graphene,³⁶ CVD growth and transfer,¹⁶ the reduction in graphene oxide,³⁷ the tailoring of graphene via etching,³⁸ and exposure of graphene to electron beam irradiation.³⁹ It has been shown⁴⁰ that stable, unpassivated, basal-plane defects in the form of Stone–Wales⁴¹ configurations and interstitial-vacancy recombination⁴² can readily exist in graphene sheets. These defects induce short-range scatters to the material, whose role is to limit mobility⁴³ at high carrier concentrations. It has been observed⁴⁴ that in the event of defect generation in vacuum, C–C reconstruction will occur rapidly, with a stable unpassivated defect site forming in a matter of seconds. The *in situ* doping method presented in this work demonstrates that by performing the graphene growth process in an environment rich with the passivating specie, passivation at the time of defect generation can lead to an efficient conversion of unpassivated defects to dopant sites, with unique opportunities for spatial selectivity. By employing *in situ* doping of edge defect sites alone, n-type carrier concentrations on the order of $1.5 \times 10^{12} \text{ cm}^{-2}$ can be observed while maintaining high mobility. Edge doping is speculated to provide a robust, long-term doping mechanism for graphene, given the energetically stable structure of an N-passivated edge. Postpassivation, the edge is predicted to become chemically inert, and provide a constant doping, excluding the breaking of N–C bonds or generation of fresh defects.

In conclusion, it is shown that *in situ* doping methods are highly attractive for the efficient incorporation of dopant species into the graphene lattice. By carrying out the exfoliation of graphene in a N-ambient, the dopant specie can play an active role in minimizing C–C reconstruction by passivating defect sites, thereby producing n-type GRs. The presence of the passivating specie at the moment of defect generation is thought to be essential to the minimization of unpassivated defect sites, whose only role is to limit graphene's mobility. *In situ* doping methods are highly attractive as counterparts to the growth and transfer processes, where natural kinetics can be exploited to provide unique avenues for the direct embedding of dopant atoms, an opportunity lacking in post-growth doping methods.

The authors acknowledge funding support from the Semiconductor Research Corporation and the Defense Advanced Research Projects Agency (DARPA) through the Interconnect Focus Center, and the National Science Foundation (ECCS: Grant No. 1001986).

- ¹K. I. Bolotin, K. J. Sikes, Z. Jiang, M. Klima, G. Fudenberg, J. Hone, P. Kim, and H. L. Stormer, *Solid State Commun.* **146**, 351 (2008).
- ²K. S. Novoselov, A. K. Geim, S. V. Morozov, D. Jiang, Y. Zhang, S. V. Dubonos, I. V. Grigorieva, and A. A. Firsov, *Science* **306**, 666 (2004).
- ³C. Berger, Z. M. Song, T. B. Li, X. B. Li, A. Y. Ogbazghi, R. Feng, Z. T. Dai, A. N. Marchenkov, E. H. Conrad, P. N. First, and W. A. de Heer, *J. Phys. Chem. B* **108**, 19912 (2004).
- ⁴A. Reina, X. T. Jia, J. Ho, D. Nezich, H. B. Son, V. Bulovic, M. S. Dresselhaus, and J. Kong, *Nano Lett.* **9**, 30 (2009).
- ⁵S. Ryu, M. Y. Han, J. Maultzsch, T. F. Heinz, P. Kim, M. L. Steigerwald, and L. E. Brus, *Nano Lett.* **8**, 4597 (2008).
- ⁶O. Leenaerts, B. Partoens, and F. M. Peeters, *Phys. Rev. B* **77**, 125416

- (2008).
- ⁷F. Schedin, A. K. Geim, S. V. Morozov, E. W. Hill, P. Blake, M. I. Katsnelson, and K. S. Novoselov, *Nature Mater.* **6**, 652 (2007).
- ⁸Y. J. Ren, S. S. Chen, W. W. Cai, Y. W. Zhu, C. F. Zhu, and R. S. Ruoff, *Appl. Phys. Lett.* **97**, 053107 (2010).
- ⁹G. Giovannetti, P. A. Khomyakov, G. Brocks, V. M. Karpan, J. van den Brink, and P. J. Kelly, *Phys. Rev. Lett.* **101**, 026803 (2008).
- ¹⁰A. Das, S. Pisana, B. Chakraborty, S. Piscanec, S. K. Saha, U. V. Waghmare, K. S. Novoselov, H. R. Krishnamurthy, A. K. Geim, A. C. Ferrari, and A. K. Sood, *Nat. Nanotechnol.* **3**, 210 (2008).
- ¹¹D. B. Farmer, R. Golizadeh-Mojarad, V. Perebeinos, Y. M. Lin, G. S. Tulevski, J. C. Tsang, and P. Avouris, *Nano Lett.* **9**, 388 (2009).
- ¹²X. C. Dong, D. L. Fu, W. J. Fang, Y. M. Shi, P. Chen, and L. J. Li, *Small* **5**, 1422 (2009).
- ¹³D. B. Farmer, Y. M. Lin, A. Afzali-Ardakani, and P. Avouris, *Appl. Phys. Lett.* **94**, 213106 (2009).
- ¹⁴X. R. Wang, X. L. Li, L. Zhang, Y. Yoon, P. K. Weber, H. L. Wang, J. Guo, and H. J. Dai, *Science* **324**, 768 (2009).
- ¹⁵X. L. Li, H. L. Wang, J. T. Robinson, H. Sanchez, G. Diankov, and H. J. Dai, *J. Am. Chem. Soc.* **131**, 15939 (2009).
- ¹⁶D. C. Wei, Y. Q. Liu, Y. Wang, H. L. Zhang, L. P. Huang, and G. Yu, *Nano Lett.* **9**, 1752 (2009).
- ¹⁷L. S. Panchokarla, K. S. Subrahmanyam, S. K. Saha, A. Govindaraj, H. R. Krishnamurthy, U. V. Waghmare, and C. N. R. Rao, *Adv. Mater.* **21**, 4726 (2009).
- ¹⁸Y. C. Lin, C. Y. Lin, and P. W. Chiu, *Appl. Phys. Lett.* **96**, 113510 (2010).
- ¹⁹A. C. Ferrari, J. C. Meyer, V. Scardaci, C. Casiraghi, M. Lazzeri, F. Mauri, S. Piscanec, D. Jiang, K. S. Novoselov, S. Roth, and A. K. Geim, *Phys. Rev. Lett.* **97**, 187401 (2006).
- ²⁰Y. Y. Shao, S. Zhang, M. H. Engelhard, G. S. Li, G. C. Shao, Y. Wang, J. Liu, I. A. Aksay, and Y. H. Lin, *J. Mater. Chem.* **20**, 7491 (2010).
- ²¹D. Estrada, S. Dutta, A. Liao, and E. Pop, *Nanotechnology* **21**, 085702 (2010).
- ²²K. Nakada, M. Fujita, G. Dresselhaus, and M. S. Dresselhaus, *Phys. Rev. B* **54**, 17954 (1996).
- ²³L. Brey and H. A. Fertig, *Phys. Rev. B* **73**, 235411 (2006).
- ²⁴M. Ezawa, *Phys. Rev. B* **73**, 045432 (2006).
- ²⁵Y. Miyamoto, K. Nakada, and M. Fujita, *Phys. Rev. B* **59**, 9858 (1999).
- ²⁶R. Ramprasad, P. von Allmen, and L. R. C. Fonseca, *Phys. Rev. B* **60**, 6023 (1999).
- ²⁷Y. Niimi, T. Matsui, H. Kambara, K. Tagami, M. Tsukada, and H. Fukuyama, *Phys. Rev. B* **73**, 085421 (2006).
- ²⁸P. Koskinen, S. Malola, and H. Hakkinen, *Phys. Rev. Lett.* **101**, 115502 (2008).
- ²⁹P. Koskinen, S. Malola, and H. Hakkinen, *Phys. Rev. B* **80**, 073401 (2009).
- ³⁰T. Wassmann, A. P. Seitsonen, A. M. Saitta, M. Lazzeri, and F. Mauri, *Phys. Rev. Lett.* **101**, 096402 (2008).
- ³¹B. Huang, M. Liu, N. H. Su, J. Wu, W. H. Duan, B. L. Gu, and F. Liu, *Phys. Rev. Lett.* **102**, 166404 (2009).
- ³²L. L. Song, X. H. Zheng, R. L. Wang, and Z. Zeng, *J. Phys. Chem. C* **114**, 12145 (2010).
- ³³S. F. Huang, K. Terakura, T. Ozaki, T. Ikeda, M. Boero, M. Oshima, J. Ozaki, and S. Miyata, *Phys. Rev. B* **80**, 235410 (2009).
- ³⁴S. S. Yu, W. T. Zheng, Q. B. Wen, and Q. Jiang, *Carbon* **46**, 537 (2008).
- ³⁵K. S. Kim, Y. Zhao, H. Jang, S. Y. Lee, J. M. Kim, J. H. Ahn, P. Kim, J. Y. Choi, and B. H. Hong, *Nature (London)* **457**, 706 (2009).
- ³⁶G. M. Rutter, J. N. Crain, N. P. Guisinger, T. Li, P. N. First, and J. A. Stroscio, *Science* **317**, 219 (2007).
- ³⁷S. Stankovich, D. A. Dikin, R. D. Piner, K. A. Kohlhaas, A. Kleinhammes, Y. Jia, Y. Wu, S. T. Nguyen, and R. S. Ruoff, *Carbon* **45**, 1558 (2007).
- ³⁸J. W. Bai, X. Zhong, S. Jiang, Y. Huang, and X. F. Duan, *Nat. Nanotechnol.* **5**, 190 (2010).
- ³⁹J. R. Hahn and H. Kang, *Phys. Rev. B* **60**, 6007 (1999).
- ⁴⁰A. Hashimoto, K. Suenaga, A. Gloter, K. Urita, and S. Iijima, *Nature (London)* **430**, 870 (2004).
- ⁴¹A. J. Stone and D. J. Wales, *Chem. Phys. Lett.* **128**, 501 (1986).
- ⁴²C. P. Ewels, R. H. Telling, A. A. El-Barbary, M. I. Heggie, and P. R. Briddon, *Phys. Rev. Lett.* **91**, 025505 (2003).
- ⁴³K. S. Novoselov, A. K. Geim, S. V. Morozov, D. Jiang, M. I. Katsnelson, I. V. Grigorieva, S. V. Dubonos, and A. A. Firsov, *Nature (London)* **438**, 197 (2005).
- ⁴⁴C. O. Girit, J. C. Meyer, R. Erni, M. D. Rossell, C. Kisielowski, L. Yang, C. H. Park, M. F. Crommie, M. L. Cohen, S. G. Louie, and A. Zettl, *Science* **323**, 1705 (2009).